BOREAS An international journal of Quaternary research

Entrainment and emplacement of englacial debris bands near the margin of Storglaciären, Sweden

PETER L. MOORE, NEAL R. IVERSON, KEVIN T. UNO, MATTHEW P. DETTINGER, KEITH A. BRUGGER AND PETER JANSSON

BOREAS

Moore, P. L., Iverson, N. R., Uno, K. T., Dettinger, M. P., Brugger, K. A. & Jansson, P. 2012: Entrainment and emplacement of englacial debris bands near the margin of Storglaciären, Sweden. *Boreas*, 10.1111/j.1502-3885.2012.00274.x. ISSN 0300-9483.

Internal structure, stable isotope composition and tritium concentration were measured in and around debris-bearing ice at the margin of Storglaciären, where englacial debris bands have previously been inferred to form by thrusting. Two types of debris bands were distinguished: (i) an unsorted diamicton band that is laterally continuous for more than 200 m, and (ii) well-sorted sand and gravel bands that are lenticular and discontinuous. Above-background tritium levels and enrichment of $\delta^{18}O$ and δD in ice from the diamicton band indicate entrainment by basal freeze-on since 1952. Isotopic enrichment and tritium-free ice in the sandy debris bands also indicate entrainment in freezing water, but prior to 1952. The lenticular cross-section, sorting and stratification of the sandy bands suggest that they were deposited englacially. The basally accreted diamicton band has been elevated tens of metres above the bed and presently overlies the englacially deposited sandy bands, suggesting that the stratigraphy has been disrupted. Three interpretations could account for these observations: (i) thrusting of fast-moving ice over slow, marginal ice uplifting recently accreted basal ice along the fault; (ii) folding near the margin, elevating young basal ice over older basal and englacial ice; and (iii) debris-band formation by an unknown mechanism and subsequent contamination of ice geochemical properties by meltwater flow through debris bands. Although none of these interpretations is consistent with all measurements, folding is most compatible with observations and local ice-flow kinematics.

Peter L. Moore (e-mail: pmoore@iastate.edu) and Neal R. Iverson (e-mail: niverson@iastate.edu), Department of Geological & Atmospheric Sciences, Iowa State University, 253 Science I, Ames, IA 50011, USA; Kevin T. Uno (e-mail: kevinuno1@gmail.com), Department of Geology & Geophysics, University of Utah, Salt Lake City, UT 84112, USA; Matthew P. Dettinger (e-mail: dettingm@email.arizona.edu), Geology Department, Carleton College, Northfield, MN 55057, USA; Keith A Brugger (e-mail: bruggeka@morris.umn.edu), Geology Discipline, University of Minnesota-Morris, Morris, MN 56267, USA; Peter Jansson (e-mail: peter.jansson@natgeo.su.se), Department of Physical Geography & Quaternary Geology, Stockholm University, SE-106 91 Stockholm, Sweden; *received 3rd February 2012, accepted 16th May 2012.*

Bands and lenses of sediment-bearing ice crop out at the margins of many modern glaciers, particularly polythermal glaciers with frozen margins (Boulton 1970; Hambrey *et al*. 1999). As ablation proceeds in debris-bearing ice margins, the released sediment can accumulate on the ice surface in patterns inherited from structures in the ice (Glasser *et al*. 1998; Evans 2009). Where such landforms are preserved at a former ice margin, these patterns have been used to infer parent englacial structures and in some cases have even been interpreted to reflect ancient climatic conditions (Hambrey *et al*. 1997). Our understanding of how such englacial debris bands form is, however, incomplete, leaving such climatic interpretations uncertain (e.g. Lukas 2005).

Debris bands are formed and emplaced englacially by various processes. In valley glaciers, some englacial debris bands contain bodies of coarse, angular sediment derived from valley-side rockfall. However, in many cases – notably in ice caps and ice sheets lacking significant supraglacial debris input – the sediment contained in englacial debris bands is ultimately derived from the bed (Boulton 1970). Many mechanisms have been suggested for entrainment from the bed and the uplift of debris bands in these environments, but few have been cited as often as thrusting. Most researchers who invoke thrusting envision fast-sliding ice moving up and over stagnant or slow-moving marginal ice in the longitudinally compressive environment of glacier termini. Despite its widespread application, the thrust model for the uplift of basal debris, and the proper criteria for field recognition of thrusts have been long debated (e.g. Weertman 1961; Hooke & Hudleston 1978; Woodward *et al*. 2002, 2003; Glasser *et al*. 2003a).

Herein, we attempt to better constrain the origin and uplift of debris bands at the margin of Storglaciären, a non-surge-type polythermal glacier in northern Sweden. Recent observations and measurements there by Jansson *et al*. (2000) and Glasser *et al*. (2003b) led to the tentative interpretation that regelation infiltration of basal debris and subsequent thrusting were responsible for the debris bands. We build on these prior measurements by considering both oxygen and hydrogen stable isotopes and by measuring tritium in and around the debris-bearing ice. These measurements indicate the relative ages of debris bands and the enclosing clean ice and provide constraints on the mechanisms of debris

DOI 10.1111/j.1502-3885.2012.00274.x

entrainment. We also leverage the model results presented in Moore *et al.* 2010, 2011) to evaluate possible uplift mechanisms.

Background

Sediment can be entrained from the glacier bed by a number of processes involving both ice and meltwater (Alley *et al.* 1997; Knight 1997). Basal sliding can incorporate diffuse basal sediment as creep, melting and refreezing allow ice to move past obstacles in the bed (Hubbard & Sharp 1995). If basal effective stress is sufficiently high, regelation infiltration can incorporate dense sediment layers a few decimetres thick (Iverson & Souchez 1996; Iverson *et al.* 2007; Rempel 2008). Meltwater moving along the ice-bed interface or in englacial fractures or conduits can freeze and capture suspended sediment if the water becomes supercooled by rapid decompression, creating diffuse or laminated debris layers (Lawson *et al.* 1998; Ensminger *et al.* 2001). Finally, where the climate is sufficiently cool that ice near the surface and at the terminus is subfreezing (i.e. in cold or polythermal glaciers), meltwater at the bed can freeze onto the glacier base as heat is lost by conduction through the ice (Weertman 1961). This final mechanism can potentially entrain decimetre- to metre-thick packages of dense debris.

Determining the process responsible for entraining a particular debris band requires knowledge of debris characteristics and of the properties of the interstitial and enclosing ice. Geochemical analysis can also help to determine the origin of debris layers. Particularly useful are stable isotope ratios of oxygen ($\delta^{18}O$) and hydrogen ($\delta^{2}H$ or, equivalently, δD), and the concentration of radioactive tritium (^{3}H).

Stable isotopes are also commonly measured in glacier ice to assess whether freezing of meltwater was involved in the sediment entrainment processes (Hubbard & Sharp 1995). Fractionation of the stable isotopes of oxygen and hydrogen accompanies the freezing of water, such that ice formed initially is enriched in the heavy isotopes compared with the source water. The isotopic composition of this meteoric source water varies with air temperature and moisture source, but typically lies along a local meteoric water line (LMWL) with a co-isotopic slope (δD vs.$\delta^{18}O$) less than ~8. Systematic deviation from the slope of the LMWL in glacier ice can indicate that the ice formed or was altered by the complete or partial freezing of meltwater (Jouzel & Souchez 1982; Souchez & Jouzel 1984). Comparison of the co-isotopic composition of debris-bearing glacier ice with the LMWL can thus constrain the debris entrainment process.

Spatial patterns in isotopic composition and the isotopic relationship between debris layers and surrounding clean ice can also help in the identification of entrainment processes. Iverson & Souchez (1996) showed that debris-rich ice formed by regelation infiltration creates a dense debris layer that becomes progressively enriched from the top of the layer to the bottom. In contrast, the freeze-on of subglacial meltwater in an ideally 'closed' subglacial system initially produces isotopically enriched ice as heavy isotopes are preferentially sequestered in the solid phase. As freezing continues, late-forming ice becomes progressively depleted along a freezing slope (Souchez & Jouzel 1984), producing an isotopic profile opposite to that from regelation infiltration. Unfortunately, the closed subglacial hydraulic system is a theoretical idealization that is probably rare in nature. Under the more realistic assumption that the subglacial hydraulic system is open and the source water composition changes over the period of accretion, the ice would not necessarily exhibit a freezing slope, nor would it necessarily show signs of progressive enrichment across the debris layer. It may, however, still be relatively enriched if the source water has an isotopic composition similar to the ice above (Souchez & de Groote 1985).

A potential difference between ice that regelates into underlying sediment and ice that freezes from basal meltwater is age. The radioactive isotope tritium, ^{3}H (half-life=12.3 a), incorporated in small amounts in atmospheric water, can be used to identify ice that contains precipitation falling after 1951 (e.g. Strasser *et al.* 1996). Natural tritium production in the upper atmosphere results from cosmic ray bombardment of nitrogen, but comparatively large amounts of tritium were introduced into the atmosphere as a result of surface thermonuclear weapons testing between 1951 and 1963. Since an international agreement banning atmospheric nuclear testing, tritium concentrations in the atmosphere have declined to near background concentrations. Background levels of tritium at high northern latitudes are as high as 12.5 TU (Kotzer *et al.* 2000). During the summer 'bomb-peak' of 1963, tritium concentration in northern Scandinavia precipitation was 5950 TU (measured 15th June 1963; Östlund & Lundgren 1964).

The use of tritium for relative age dating in ice requires accounting for the decay of tritium to its daughter product, ^{3}He. Pre-bomb precipitation in 1950 containing 12.5 TU would contain only 0.48 TU after 58 years of decay, and older ice would contain still less as the age of the ice increased. Hence, 0.5 TU represents a reasonable maximum value for pre-bomb ice. For glaciers large enough that ice residence times are hundreds or thousands of years (this includes Storglaciären), glacial ice regelating into the bed near the terminus should be effectively free of tritium. Ice formed after 1951 could have higher tritium concentrations, up to about 469 TU for ice formed from precipitation in 1963 (assuming an initial 5950 TU). There-

fore, tritium concentrations larger than 0.5 TU in ice can be taken to indicate that at least some fraction of the ice was formed from water that condensed in the atmosphere after 1952 (Strasser *et al*. 1996).

Some mechanisms of sediment entrainment can directly emplace the debris englacially, whereas others require uplift after entrainment. Examples of the former group include basal (Woodward *et al*. 2002) or surface crevasse fills, injection of sediment and supercooled water into basal crevasses (Ensminger *et al*. 2001), and the preservation of water-lain sediment deposited in englacial conduits (Kirkbride & Spedding 1996). Debris emplaced well above the glacier bed by these mechanisms will often be surrounded by geochemically 'pristine' glacier ice, probably tritium-free and isotopically depleted. Most of the remaining common entrainment processes accrete sediment to the glacier sole, so that debris is brought to the surface only after uplift and perhaps stratigraphic disruption. The geochemical signature of ice surrounding basally entrained debris depends on the detailed thermal history of the basal ice zone and the mode of uplift.

Uplift of basal ice is thought to occur through bulk thickening, folding or thrusting (Alley *et al*. 1997). Each of these processes requires a compressive stress regime, usually in the longitudinal (flow-parallel) direction. Bulk thickening is simply the homogeneous vertical extension that accompanies longitudinal shortening when transverse extension is inhibited (Weertman 1966). This is manifested as upturned flowlines that can bring basal debris passively to the surface without heterogeneous strain, and has been inferred from field observations (Hooke & Hudleston 1978) and shown theoretically (Hooke & Hudleston 1978; Moore *et al*. 2009). Uplift by bulk thickening does not require stratigraphic disruption, and any exposure of basal ice at the glacier surface should therefore be underlain by more basal ice and be progressively younger with depth. In contrast, folding and thrusting do necessarily entail stratigraphic disruption and may therefore result in repeated or overturned strata and the juxtaposition of ice and sediment facies formed in different englacial or basal environments. Folding or thrusting, or a combination of both processes, may thus be responsible for the appearance of debris layers of basal origin overlying englacial ice of meteoric origin. An extensive body of literature (e.g. Hambrey *et al*. 1999; Evans 2009; Benn & Evans 2010) describes the field identification of thrusts, usually on the basis of offset structures, ice crystal fabrics, or bands of basally derived debris in locations and orientations consistent with longitudinal compression. Fewer studies have discussed folding and its contribution to debris uplift, and it is often inferred to occur as a predecessor to thrusts (Clarke & Blake 1991; Glasser & Hambrey 2002; Swift *et al*. 2006).

Field setting

Storglaciären is a 3-km-long polythermal valley glacier in northern Sweden with a rich history of glaciological measurements (Fig. 1). Most of the glacier ice is temperate except for a surface layer 20–70 m thick in the ablation zone that is below freezing (Pettersson *et al*. 2007). This cold surface layer meets the bed within ~50–150 m of the terminus according to radar and thermistor measurements (Moore *et al*. 2011). The temperate-based ice upglacier is known to undergo basal motion by both sliding and bed deformation (Iverson *et al*. 1995; Moore *et al*. 2011). Measurements by Moore *et al*. (2011) indicate that basal motion unexpectedly continues beneath the cold-based terminus, perhaps at depth within a deformable sediment layer. Near the centre of the terminus where the ice surface and bed slope down-glacier, this weak substrate limits longitudinal compression. However, in the northern portion of the terminus, the glacier bed has a gentle adverse slope where it encounters a small moraine mound (Fig. 2). In 1994 an ice-cored ridge appeared at the surface on the northern side of the terminus (Jansson *et al*. 2000). This ice-cored sediment ridge and the associated debris bands have remained exposed at the glacier surface since then, although in 2008 the outcrop was within a few metres of the ice margin. Several debris layers have been recognized in the area of the debris ridge by previous workers (Glasser *et al*. 2003b). The most prominent band crops out for ~200 m and roughly parallels the ice margin from the northern edge of the terminus to about 30% of the way south across its width. This band's exposure approximately coincides with the extent of the moraine mound in the glacier forefield. The debris band varies from about 10 to 40 cm in thickness, dips upglacier to the southwest between 31° and 70° (decreasing toward the south, or glacier centreline), and consists of poorly sorted, subangular to subrounded sediments, primarily sand

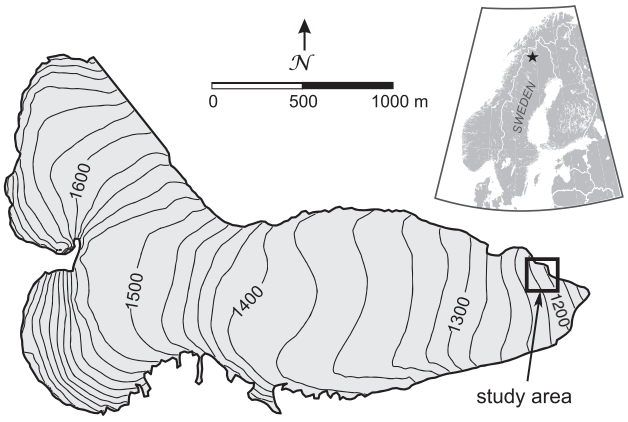

Fig. 1. Contour map of Storglaciären (m a.s.l.).

Fig. 2. Photo of the study area, taken in 2007 from the north, showing the distinct debris ridge near the margin. A small moraine mound is visible in the middle-ground on the left side of the photo, extending from the meltwater stream (Nordjokk) on the near side to an ice-marginal snow field in the middle of the terminus. The white box shows the approximate extent of the map in Fig. 3.

and gravel. Sediment concentration varies from 45% to more than 75% by volume (Glasser *et al.* 2003b; Uno 2008; Moore 2009). Stable oxygen isotope measurements of Glasser *et al.* (2003b) suggested that the sediment was entrained from the bed by regelation infiltration prior to uplift to the surface, but their results could not constrain how far upglacier of the terminus this entrainment took place and therefore could not constrain the timing of debris band uplift.

Jansson *et al.* (2000) observed englacial reflections in ground-penetrating radar (GPR) surveys that appeared to represent the continuation at depth of the primary debris band that crops out at the surface. Projection of this reflection towards the glacier bed suggested that it emanated from the transition between warm-based and cold-based ice (the basal thermal transition), and further suggested that entrainment may have occurred near this thermal transition. Jansson *et al.* (2000) also found that the surface outcropping of this feature coincided with a significant decline in glacier surface velocity. These observations, combined with sedimentological analysis of the debris, led Glasser *et al.* (2003b) to conclude that the terminus of Storglaciären was under substantial longitudinal compression and that this compression was accommodated by thrust faulting and the displacement of dirty basal ice to the surface. However, oxygen isotope measurements in and around the debris band did not fully corroborate the inferred entrainment mechanism. Additional questions also remained regarding how thrust displacement might have been accommodated within or adjacent to the debris layers (Glasser *et al.* 2003b).

Methods

Outcrops of the Storglaciären debris bands were investigated and sampled during the summers of 2006, 2007 and 2008. The location of the surface expression of the most extensive debris band was measured in 2007 using a Trimble (4600 LS receiver and 4000 SSI base) differential GPS. Where the *in situ* debris bands were covered with accumulated debris, outcrops were mechanically and hydraulically cleaned for visual inspection and description. Layer orientations were measured with a Brunton compass, and thicknesses with a tape measure. Ice facies were described first as either debris-bearing or clean, and then further classified according to the scheme of Hubbard & Sharp (1995). Longitudinal sections along supraglacial melt streams provided exposures for measurement of band thicknesses and attitudes. Sediments in the debris-bearing ice were described qualitatively (both in outcrop and after debris-bearing samples were melted) according to their composition, texture, grain roundness and sedimentary structures. The deeper subsurface orientation of the most widespread debris band was investigated englacially using a Heucke steam drill in 2007. Whereas a high-pressure hot-water drill used for drilling instrumentation boreholes was able to penetrate slowly through decimetre-thick englacial debris bands, the steam drill could not. Therefore, the depth to the debris band was inferred to be the depth at which downward melting with the steam drill was halted. The total length of the drill stem and drill hose was 10 m, thus limiting the probing depth. A network of 18 steam-drill holes was drilled in 2007 in the ice just upglacier from the surface expression of the debris band.

Samples of ice were obtained from within and immediately surrounding the debris bands in 2006 and 2008 for stable isotope and tritium analysis (Fig. 3). For reference, samples of young bubbly ice were also collected from the ice surface just below the equilibrium line, and water was sampled from each of the two major meltwater streams issuing from the glacier terminus (Nordjokk and Sydjokk). To minimize contamination from surface meltwater, ice was removed from the exposure with a sledgehammer and chisel or a chainsaw to access uncontaminated ice at least 20 cm beneath the surface. Samples were either chipped from the outcrop with a chisel or extruded through an ice screw. Ice and all included sediment were collected from each sample site so that debris contents could be computed in the laboratory from the mass fractions of melted ice and sediment. Ice for both stable isotope and tritium analysis was stored for transport in polyester bottles sealed with parafilm. Volumetric debris concentrations in debris-bearing ice were computed from measurements of oven-dried sediment and meltwater mass assuming a uniform rock density of 2700 kg m^{-3}.

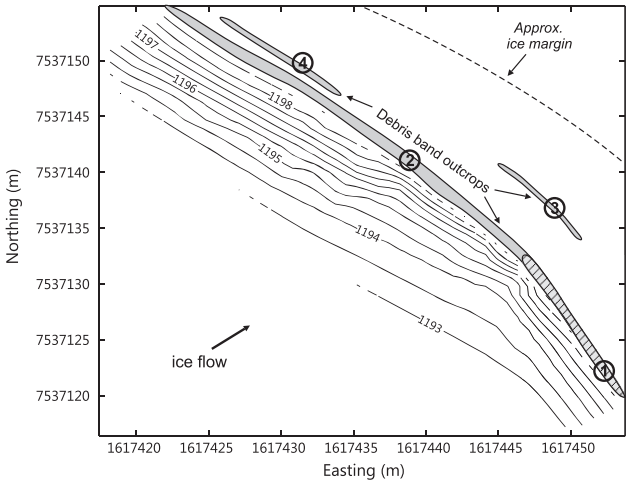

Fig. 3. Map of the southern portion of the debris band outcrop and approximate ice sampling locations. The cross-hatched portion of the debris band was not visible at the surface until 2008, although it was encountered in 2007 beneath the surface when the area was probed with a steam drill. The location of the major debris band containing sample sites 1 and 2 was determined in 2007 with differential GPS, while debris bands for sites 3 and 4 are approximate values for 2007. Contours represent the subsurface position of the debris band as interpolated from 18 steam drill holes in 2007. Further steam drilling to the south and east along-strike of the area mapped did not intersect any debris bands to ~9 m depth. Map coordinates are the Swedish grid RT90 2.5gV. Contour lines in m a.s.l.

Stable isotope analysis of δD and $\delta^{18}O$ was performed at the University of Utah (Stable Isotope Ratio Facility for Environmental Research) using a thermochemical elemental analyzer coupled to an isotope ratio mass spectrometer. Debris was removed with a 0.4-micron filter prior to analysis to remove solids from debris-bearing ice. Isotope ratios were measured at least four times per sample to improve measurement precision. Analytical uncertainty was 0.5' for δD and 0.1' for $\delta^{18}O$.

Tritium concentration was measured at the Dissolved Gas Laboratory at the University of Utah using the 'helium ingrowth' method described by Clarke *et al.* (1976). Water melted and filtered from an ice sample was extracted into an evacuated stainless steel ampule, degassed, and allowed to sit for 30–120 days (depending on water volume) to permit ^{3}H decay. Tritiogenic ^{3}He concentration was then measured with a MAP-215 noble gas mass spectrometer. To eliminate error arising from contamination with non-tritiogenic ^{3}He (e.g. by leakage of the ampule or incomplete degassing of atmospheric helium), ^{4}He was also measured. Samples containing greater than the detection threshold of ^{4}He were degassed and held again for re-analysis.

Results

The debris bands appear to be of two different types, judging from the extents of the various debris bodies and the texture of the sediments they contain. The most prominent band – the one that controls the location of the ice-cored ridge – is predominantly a coarse, poorly sorted diamicton layer ranging from 10 to 25 cm thick (Fig. 4). Particles are subangular to subrounded, occasionally striated or faceted, and of mixed lithologies. Within the diamicton layer, centimetre-scale pockets of clear ice, elongated parallel to the band, are common. The upper and lower boundaries of the band are irregular on a centimetre scale, but sharp. Along its outcrop, the band bifurcates in at least one place and appears to become two bands, separated by a thin wedge of coarse, clear ice. The debris content of the diamicton band is ~45–50% by volume. The second type of band crops out in various places a short distance (0–5 m) down-glacier from the diamicton band (sites 3 and 4; Fig. 5). Exposures are not laterally continuous over distances of more than 10 m, and in places they pinch out abruptly at a rounded edge (Fig. 5A). This second type of band has volumetric debris concentrations ranging from 55 to 70%. The debris is primarily well-sorted sand with lenses of gravel (Fig. 5B), and, where present, the gravel typically lies above (up-glacier from) the sand. In contrast to the diamicton band, no intercalated pockets of clear ice are present. The boundaries of the band are wavy but sharp, and the surrounding ice is clear and coarse. Ice within a few centimetres above and below the debris bands is coarse-grained and

Fig. 4. View to the northwest along-strike of the major debris band and associated ice-cored debris ridge near Site 2 in 2007. An *in situ* outcrop of this debris band can be seen beneath the shovel handle. Debris band thickness (~25 cm) and up-glacier dip (~60°) can be seen where a supraglacial stream has incised in the foreground.

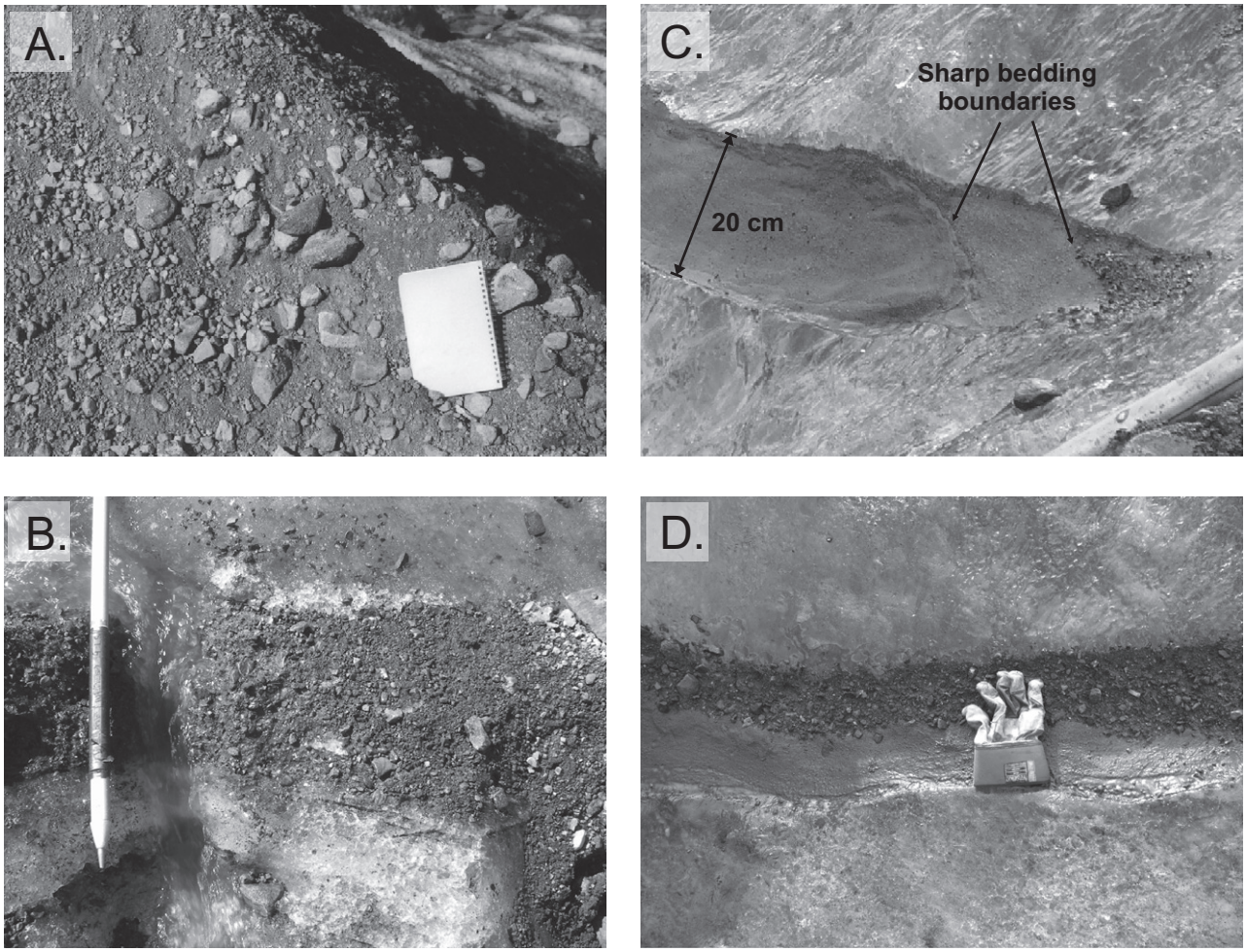

Fig. 5. Close-up photos of debris bands and supraglacial sediment accumulation. A. Loose sediment melted out from the diamicton debris band accumulating at the crest of the ice-cored debris ridge near Site 2, showing subrounded and subangular pebble- and cobble-sized clasts in a finer sandy matrix. Field notebook is 18 cm tall. B. Close-up photo of the diamicton debris band in an exposure on the southern end of the ice-cored ridge (near Site 1 of Fig. 3). Ice axe grip is ~20 cm long. C. Northern edge of a sandy band outcrop at Site 4, showing the rounded band margin and internal bounding surfaces suggesting scouring or concentric (edge to middle) layering. D. Approximately 2 m south along the same band as above, showing gravel overlying well-sorted sand, suggesting inverse grading. Glove is ~18 cm long. Photos B–D were taken facing up-glacier and looking down on outcrops sloping toward the glacier margin.

clear, but coarse bubbly layers of clean ice can be found both up-glacier and down-glacier of the debris bands. At the ice surface all of the bands are approximately parallel to one another and to local foliation, dipping up-glacier between 31° and 70° and with dips increasing along-strike towards the northern lateral margin.

Subsurface investigation with the steam drill reveals that a continuous debris layer (Fig. 3) does indeed dip up-glacier and towards the centreline. The dip is steepest near the surface (as high as 70°) and becomes gentler with depth (24°), particularly towards the southern extent of the band. Probing in 2007 indicated that the band continued at depth some distance to the south of where its outcrop disappeared. This was confirmed in 2008, as ablation exposed ~10 m of outcrop along-strike to the south of where it was visible in 2007 (hatched area in Fig. 3). However, radar profiles and borehole video inspection of the area indicate that the feature does not continue as far south as the glacier centreline (Moore 2009). The debris band thus appears to be limited to the portion of the terminus abutting the small moraine mound (Fig. 2) on the northern edge of the ice margin.

In general, debris-band ice from both types of band is isotopically enriched compared with most of the surrounding clean ice (Fig. 6). There is substantial overlap between the clear and debris-rich ice samples (Fig. 6B, C), but a Student's *t*-test indicates that the two populations are statistically distinct at the 95% confidence level (p=0.0025 for δD, p=0.00064 for δ^{18}O). A linear regression of the entire data set gives a line with a slope

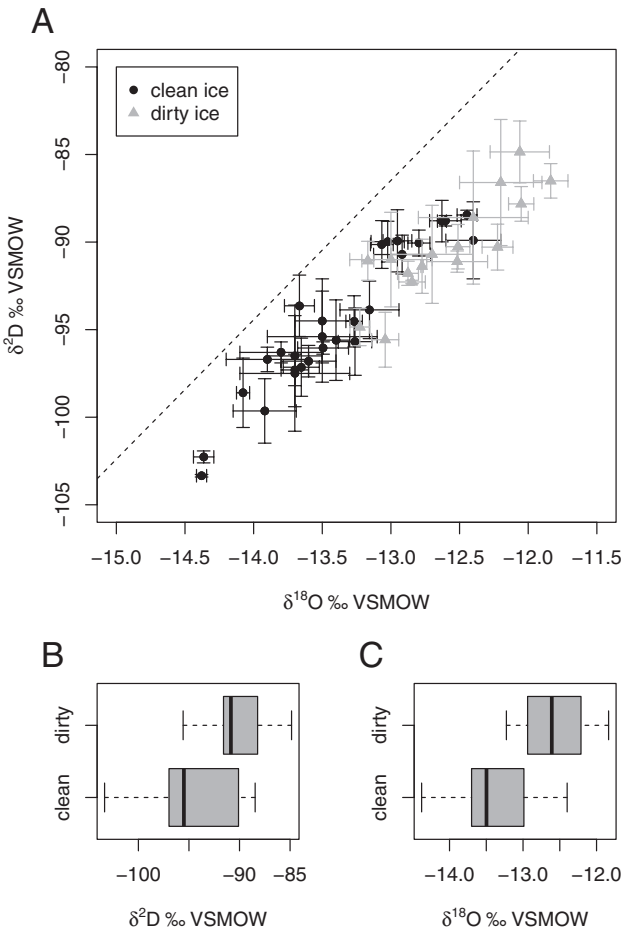

Fig. 6. Stable isotope compositions of debris-bearing ('dirty'; grey triangles) and clean (black circles) ice from the vicinity of the debris bands. A. Co-isotopic scatter plot showing the oxygen and deuterium isotopic composition of ices compared with the local meteoric water line (LMWL, unpublished data, P. Jansson). All values are per mil (‰) relative to the VSMOW, and error bars show 2σ uncertainty bounds. Box plots in (B) δD and (C) $\delta^{18}O$ illustrate the differences between population quartiles and median values.

of 6.2, but heterogeneity from one site to another suggests that this composite slope may not represent a robust pattern (Fig. 7).

Profiles across individual debris band exposures do not exhibit uniform spatial patterns of enrichment or depletion (Fig. 7). A possible trend towards progressive depletion from the top of the debris to the bottom at Site 1 (with a co-isotopic slope of 6.59) is not matched in the profile from the same band at Site 2 (here we use 'top' and 'bottom' loosely to refer to the up-glacier and down-glacier directions across the outcrops). A striking discontinuity in the isotopic composition appears in the clean ice across the debris band at Site 2. Ice below the band at this site is among the most isotopically depleted in the area. However, the same is not true below the same band at Site 1, where the isotopic composition is similar to that of other clean ice. Ice in the sandy bands is consistently enriched compared with surrounding clean ice, and no discontinuities are apparent across the bands.

Tritium concentrations of debris-rich ice, surrounding clean ice, young bubbly ice and the meltwater streams are compared in Fig. 8 and shown in Table 1. Only in the clear ice are tritium concentrations consistently near zero, although three of four debris-rich ice samples from sandy bands are also nearly zero. The fourth sandy ice sample, collected less than 1 m away from one of the tritium-free samples, had a tritium concentration of 3.3±0.4 TU. Three separate analyses from this sample yielded the same result, so measurement error is unlikely, indicating that tritium heterogeneity in the sandy band is real. In contrast, the diamicton band had a fairly consistent tritium concentration of ~1 TU (Fig. 8). Recent glacier ice (represented by the 'young bubbly ice' sampled from near the equilibrium line) appears to have a concentration of ~3.2 TU, but changing temperatures and meteoric water sources can cause tritium concentrations to vary in time and space, so this value is not necessarily representative of modern meteoric precipitation. Indeed, a sample of rainwater collected in 2006 in nearby Kiruna, Sweden, had a concentration of 12 TU (Uno 2008). The northern meltwater stream, Nordjokk, which receives surface melt from the accumulation area (Seaberg *et al.* 1988), had consistently higher tritium concentrations (~5.7 TU) than Sydjokk (~3.4 TU), which drains the upper ablation area. The tritium measurements are summarized in Fig. 8 and compared with projected decay curves for ice formed from precipitation in Ottawa, Canada, using tritium data from Clark & Fritz (1997).

Discussion

The sandy debris-rich layers exhibit lenticular structure, grain sorting and a clast-supported framework, indicating that they contain sediment transported and deposited by water. Sedimentary structures near the margins of the bands show that entrainment occurred in englacial passages. An apparent coarsening upwards appears in the band at Site 4, suggesting inverse grading or overturned normal grading. The stable isotope composition of the debris-bearing ice is isotopically enriched compared with most of the clean ice surrounding the bands, suggesting that freezing of interstitial water was responsible for 'locking' the debris in place once deposited. However, the fact that only one sample from these bands contains considerably more than 0.5 TU of tritium suggests that they may have been entrained prior to 1952. The high tritium measurement (3.7 TU) in one sample was probably not in error because three independent analyses yielded similar values, so a physical explanation for the anomalous

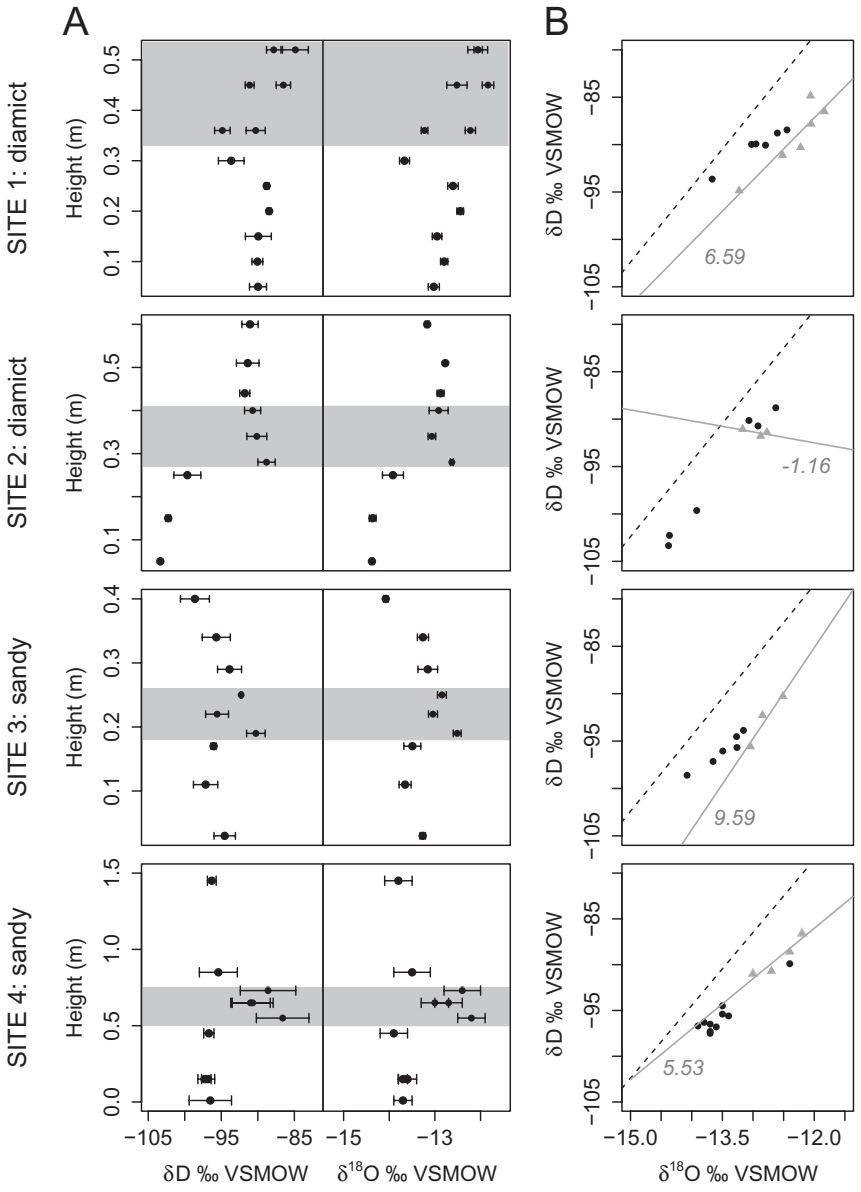

Fig. 7. Stable hydrogen and oxygen isotopes at each sample site shown in Fig. 3. A. Isotopic profiles across the debris-band outcrops. The length scale on the vertical axis is in metres along the sloping ice surface from an arbitrary datum, increasing up-glacier. Shaded regions are debris-bearing ice. The lowest samples at Site 4 were collected ~2 m down-glacier from the debris band but are shown at 0 m for simplicity. B. Co-isotopic plots at each site shown in (A). As in Fig. 6, black circles are clean ice samples and grey triangles are debris-bearing ice samples. The dashed black lines are the LMWL of Fig. 6, while the solid grey lines are least-squares regressions for the dirty ice samples. Grey numbers next to these lines are the best-fit slope to the regression. Error bars have been omitted to improve the visibility of patterns. No samples were collected above the debris band at Site 1 owing to meltwater pooling there during sampling. All isotopic values are per mil (‰) relative to VSMOW.

measurement is required. Recalling that drilling through englacial debris bands occasionally tapped an englacial water conduit, a reasonable interpretation is that portions of some debris bands have been exploited as permeable passages for young meltwater in the recent past, thus introducing tritiated water into structures that were formed prior to the bomb-peak. An alternative interpretation is that the debris-band sediment was entrained recently with young water and subsequently contaminated in most places with water derived strictly from melt of older ice. The latter interpretation is rejected because we find it unlikely that recent basal meltwaters near the terminus could exclude some contribution from young meteoric water sources (e.g. snow-melt). If the tritium concentrations measured in marginal meltwater streams are indicative of the composition of the subglacial meltwater that would be available for freeze-on (Seaberg *et al.* 1988), such young water should contain much more than 0.5 TU. Therefore, the sandy bands are interpreted to be preserved conduits formed prior to 1952 by the hydraulic transport of sediment and subsequent (or penecontemporaneous) freezing of water.

The diamicton in the main debris band closely resembles a coarse till in texture and clast induration, consistent with entrainment by accretion from the bed. Tritium concentrations greater than 0.5 TU indicate that the debris is enclosed in young ice, and therefore probably not by regelation infiltration of old tritium-free englacial ice. Clear ice lenses, a slight enrichment in stable isotopes and the lack of a consistent spatial pattern in the isotopic profiles further indicate that

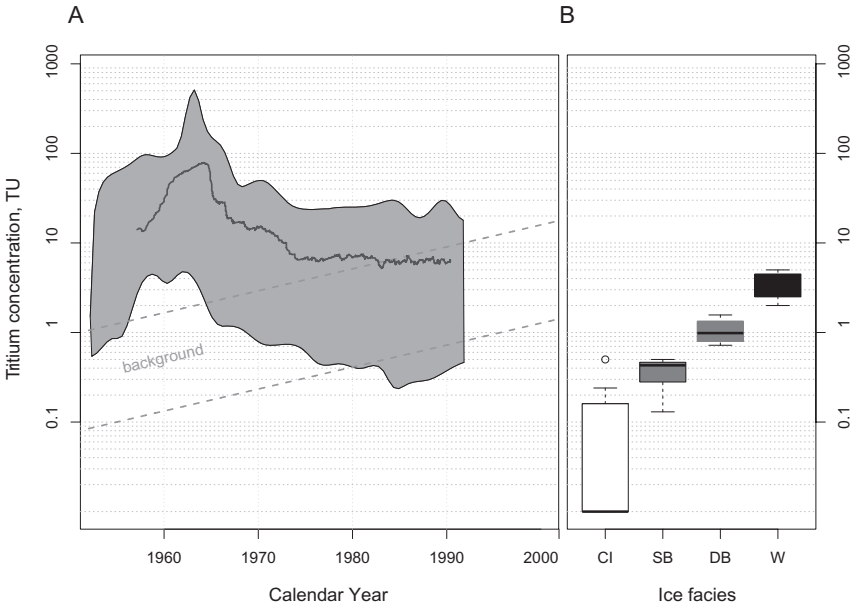

Fig. 8. Decay-corrected tritium (A) projections and (B) measurements from Storglaciären ice and water samples collected in this study. Historical tritium data in (A) comes from an extensive data set from Ottawa, Canada, precipitation in Clark & Fritz (1997). For simplicity, a shaded envelope was visually fitted around all but the extreme outliers and the thick grey line shows a smoothed mean. Precipitation measurements in 1962–1963 from Kiruna, 45 km east of Storglaciären, fall within or above the Ottawa envelope, reaching as high as 1387 TU (Östlund & Lundgren 1964). Decay correction was computed assuming $C_{2008}=C_{t0}\exp[-\lambda(2008-t_0)]$. Projected background values are computed assuming background tritium in the range 3–20 TU. Abbreviations on the horizontal axis in (B) are: CI = clean ice; SB = sandy band; DB = diamicton band; W = meltwater streams. The outlier from the sandy band data set has been omitted from (B) for clarity.

open-system basal freeze-on was the entrainment mechanism. A steep basal temperature gradient measured closer to the glacier centreline was interpreted by Moore *et al.* (2011) to result from latent heat liberated by basal freezing. Because the ice in this band is fairly uniformly tritiated – albeit at low concentrations – this entrainment presumably occurred recently. Alternatively (as above), the tritium could have been introduced after entrainment by water passing through the pore spaces and replacing the water originally involved in entrainment. However, the introduction of a tritium signal that is spatially nearly uniform by contamination with meltwater would be surprising. Furthermore, melting of the original interstitial ice by contaminating water would probably remove ice lenses and allow compaction of the sediment framework, leaving the debris more densely packed than the 45–50% (sediment volume fraction) measured. Therefore, we assume that the tritium and stable isotope data from the diamicton band retain the original geochemical signatures, indicating recent entrainment by basal freeze-on. This result contrasts with the conclusions of Glasser *et al.* (2003b), who argued that the bands were entrained by regelation infiltration based on a more limited set of $\delta^{18}O$ data.

Table 1. Tritium in Storglaciären ice and water.

Sample no.	Ice facies	^{3}H conc. (TU)	±2σ
1DB1	Diamicton	0.9	0.2
1DB2	Diamicton	1.1	0.3
2DB1	Diamicton	1.6	0.6
2DB2	Diamicton	0.7	0.4
3DB1	Sandy	0.1	0.2
3DB2	Sandy	0.4	0.2
4DB1	Sandy	0.3	0.3
4DB2	Sandy	3.7	0.6
1BDB1	Clear	0.1	0.1
1BDB2	Clear	0.2	0.1
4ADB1	Clear	0.0	0.3
4ADB2	Clear	0.0	0.3
4BDB1	Clear	0.0	0.1
4BDB2	Clear	0.5	0.3
4BDB3	Clear	0.0	0.4
4BDB4	Clear	0.0	0.2
YBI1	Young ice	3.0	0.4
YBI2	Young ice	3.2	0.4
Nord06	Nordjokk	5.6	1.0
Nord08	Nordjokk	5.9	0.5
Syd06	Sydjokk	3.4	0.7
Syd08	Sydjokk	3.8	0.4
Kiruna	Rainwater	12.0	0.9

The geochemical data indicate that the two types of debris bands were entrained by different processes and in different positions relative to the glacier bed and margin. The sandy bands were probably entrained prior to 1952 as subglacial water entered englacial passages or fractures, transporting and depositing sand and gravel with it. Hooke *et al.* (1988) hypothesized that basal meltwater could be diverted englacially over basal overdeepenings owing to the freezing of supercooled water on adverse bed slopes and the consequent clogging of basal meltwater passages. Several well-documented overdeepenings in the bed of Storglaciären could account for the diversion of basal water and sediment into englacial passages. The resulting sand and gravel bodies were above the bed and probably close to bed-parallel at the time of formation. The diamicton debris band was later entrained at the bed a short distance from the terminus, perhaps close to the basal thermal transition. Unless there has been a large localized displacement between the bands, the diamicton band was originally parallel to and below the sandy bands.

Where it was exposed at the glacier margin in 2008, the diamicton band dipped up-glacier and overlaid ~10 m of clear and dispersed facies ice containing some sandy debris bands. Therefore, if our interpretations of the entrainment process and timing are correct, not only have the debris bands been elevated from the bed and rotated from subhorizontal, but the stratigraphy at the time of formation has been inverted in the process. The remainder of this section discusses possible scenarios for accomplishing this disruption of stratigraphy.

Mechanism of uplift and stratigraphic disturbance

The debris bands, initially formed at or near the bed, now dip up-glacier and overlie several metres of tritium-free clean ice. Sandy bands are presently found down-glacier from, and therefore stratigraphically below, the younger diamicton band. This apparent overturning of stratigraphy requires an explanation that is consistent not only with the observations described above, but also with available measurements of ice kinematics (Moore *et al.* 2011). Three interpretations are considered: (1) the uplift and overturning of stratigraphy by folding; (2) the uplift of the younger basal diamicton over older basal ice by thrusting; and (3) geochemical contamination of the debris layers. Folding and thrusting are commonly invoked in such circumstances, including in the investigation by Glasser *et al.* (2003b) of these same debris bands. The third case represents a null hypothesis that our isotopic and tritium measurements do not accurately preserve evidence of the entrainment process and therefore cannot constrain uplift.

The time frame for entrainment indicated by tritium in the diamicton debris band provides some constraints on how quickly the debris travelled from the bed to the surface. The maximum transit time between entrainment at the bed and sampling at the surface is 56 years (1952 to 2008). However, the debris bands were exposed at the surface as early as 1994, allowing a maximum of 42 years for transport to the surface (Jansson *et al.* 2000). In 30-m-thick ice (the 1995 ice thickness at the middle debris band reflection in fig. 3B of Jansson *et al.* 2000), this requires a minimum uplift rate of 0.71 m a^{-1}. The maximum local vertical velocities at the ice surface are ~1 m a^{-1} within 50 m of the ice margin in 1995 (Jansson *et al.* 2000) and 2007–2008 (Moore *et al.* 2011). This high upward vertical velocity is primarily a consequence of enhanced longitudinal compression in the northern part of the terminus and is absent closer to the centreline.

If thrusting elevated, rotated and translated the diamicton band in the time frame discussed above, surface observations and velocity measurements should be compatible with such discrete motion. For a fault dipping ~30° up-glacier, an average fault-slip rate of (30 m/sin 30°)/42 a=1.4 m a^{-1} would just suffice to bring newly accreted tritium-bearing basal ice to the surface. This fault displacement would require the ice up-glacier of the fault to move vertically 0.7 m each year relative to the ice down-glacier and would further necessitate enhanced ablation on the hanging wall to make it escape detection as a hanging-wall escarpment or a growing surface bulge. There are no such ice surface bulges or escarpments on the northern portion of Storglaciären's terminus, nor have any been documented in either the literature or local records despite yearly field efforts on Storglaciären beginning in 1946. Furthermore, an attempt in 2008 to measure slip offset englacially across 1.5 m of ice enclosing the diamicton debris band yielded no displacement (Moore *et al.* 2011).

The structural concordance of all of the debris bands and with prominent foliation is also difficult to reconcile with thrusting (Jansson *et al.* 2000; Glasser *et al.* 2003b). Weertman (1961) argued that thrusting should rotate hanging-wall structures to increasing up-glacier dips while leaving footwall structures largely untilted. The result, in outcrop, should be systematic discordance between any previously subparallel structures across the fault that pre-dated the thrust (as described in, for example, Woodward *et al.* 2002). No systematic discordance between foliations or debris layers is present in the descriptions of Jansson *et al.* (2000) or Glasser *et al.* (2003b), nor was any apparent during our observation period in 2006–2008.

An alternative to thrusting that to some extent alleviates some of these problems is folding. Recumbent or overturned folds are occasionally invoked to account for many of the same structures as thrusting, and are also sometimes cited as predecessors to thrusting (Swift *et al.* 2006). To explain the observed stratigraphic relationships, the debris bands and basal ice that we observe must be within the down-glacier limb of a tight, overturned fold. Indeed, if the sandy band at Site 4 (Figs 3, 5C, D) was initially deposited with normal grading (i.e. sand was deposited on top of gravel), one can infer that it is presently overturned.

Unlike thrusting, the expression of folding in surface velocity does not involve discontinuities or escarpments but can be manifested as a smooth undulation in vertical velocity. A more challenging kinematic issue raised by the fold hypothesis is how folding that involves basal ice is accommodated at the glacier base. If a stiff, dense debris layer at the base of the glacier buckles, a cavity or void is probably opened up at the bed unless something fills the space or the fold core is very tight. Clarke & Blake (1991) considered a similar problem at Trapridge Glacier and suggested that a mound of sediment beneath the incipient fold axis could allow such a structure to develop. While those authors had no evidence for such a structure, Moore

(2009) and Moore *et al.* (2011) identified a strong, gently down-glacier-dipping radar reflection above the mean bed level just up-glacier from the ice-cored debris ridge at Storglaciären. Based on apparent radar reflection power, Moore (2009) inferred that this structure was composed of water-saturated sediment, which is known to underlie large areas of the glacier (Brand *et al.* 1987).

The possibility that our isotopic measurements represent contamination from meltwater rather than tracers for the timing and processes of entrainment deserves further consideration. Two boreholes drilled in the area for a related project (Moore *et al.* 2011) gushed turbid water for a period of hours to days when the drill intersected a debris layer englacially. It is therefore possible that portions of debris bands were occasionally exploited as meltwater conduits. As indicated previously, the 3.7-TU sample of sandy-band ice from Site 4 (Table 1) may have been contaminated in this way. If water in the outwash streams is taken to be isotopically representative of the subglacial and englacial water near the terminus (Table 1), contamination may be expected to introduce tritium concentrations in the range 3–6 TU. Contamination by water of this composition cannot account for tritium concentrations near zero in the sandy bands but could explain the anomalously high measurement at Site 4. Consistently low-level tritium values (~1.1 ± 0.4 TU) in the diamicton band would require partial contamination of the same fraction of the ice in each sample, which is unlikely. Furthermore, melting and replacement of interstitial ice in the diamicton band would probably have eliminated ice lenses, assuming that subsequent freezing of pore water occurred sufficiently rapidly to prohibit significant ice segregation. Therefore we reject the hypothesis that the majority of our dirty ice samples were contaminated by meltwater flow that post-dated debris-band formation.

None of the above uplift and stratigraphic disruption hypotheses fully explains our observations and measurements. Post-entrainment isotopic contamination of our sampled dirty ice may have occurred in at least one sample described above, but contamination would be expected to introduce younger tritiated ice into older structures rather than the converse. Thus, contamination cannot explain the apparent age difference in the debris bands. We therefore accept that there is an age difference between sandy and diamicton debris bands, and seek to explain their stratigraphic inversion physically. Thrusting requires mechanical conditions unlikely to arise at Storglaciären (Moore *et al.* 2009, 2010, 2011). Furthermore, the kinematic implications of the necessary thrust displacement rates inferred from the young diamicton band are not consistent with measurements and observations reported here or in prior work (e.g. Moore *et al.* 2011). Folding can potentially account for uplift and stratigraphic disturbance much like thrusting, and is more consistent with the expected mechanical behaviour of ice under high confinement and low strain rates. We therefore tentatively suggest that the debris bands and associated ice-cored debris ridges at Storglaciären were formed by folding near the terminus, bringing young debris-bearing basal ice layers to the terminus and locally overturning the ice stratigraphy.

Conclusions

The field observations and isotopic data presented above point to distinct entrainment mechanisms for two types of debris bands found on the north margin of Storglaciären. Sediment texture and isotopic enrichment in a diamicton-bearing debris band was probably entrained at the glacier bed by freeze-on in a hydraulically open subglacial till aquifer. Uniformly elevated tritium concentrations in this debris band indicate that entrainment and uplift occurred after thermonuclear testing began in 1952. Several sorted sand and gravel lenses were entrained englacially, prior to the weapons-testing era, by meltwater flowing through subhorizontal fractures or conduits in the ice. After deposition and freeze-in of the sediment, portions of these bands may have been exploited by meltwater flow, locally introducing a post-1952 geochemical signature to some of the debris-bearing ice, but not completely obliterating the isotopic signature of entrainment. After entrainment, these debris bands were uplifted and rotated, and in the process their original stratigraphy was disrupted.

There is no evidence of discrete displacement across the debris band at present, nor are there any past kinematic observations consistent with the magnitude of thrust displacement necessary to bring basally derived sediment to the ice surface in the time frame constrained by tritium measurements. Therefore, thrusting is rejected as the primary mechanism for exposure of these debris bands at the ice surface. Uplift and overturning by folding, though a poorly understood process in the present context, is more consistent with observations and measurements at the terminus between 1995 and 2008. However, a mechanical framework for fold development in debris-bearing glacier termini is required to fully evaluate this hypothesis.

Our results have broader implications for the interpretation of debris-band structures and properties in other glaciers. The use of tritium to provide time constraints on the uplift of basally derived debris to the surface provides lower bounds on the rate of debris uplift and thus allows testing of debris emplacement mechanisms against other direct measurements. This approach highlights the importance of considering the kinematic implications of conceptual models of glacial structure development. In addition, anomalous tritium results and borehole-drilling records suggest that

caution is needed in the interpretation of geochemical signatures preserved in debris-bearing ice because they can be profoundly altered if the structure acts as a passage for porous meltwater flow after entrainment.

Acknowledgements. – We thank Rickard Pettersson, Denis Cohen, Tom Hooyer, John Byers and Mark Mathison for assistance in the field. We also thank Henrik Törnberg and the Tarfala Research Station for providing field logistical support, and Sarah Titus, Thure Cerling, Kip Solomon and the Dissolved and Noble Gas Lab at the University of Utah, and Alan Rigby for contributions to the design and analysis of our measurements. We thank Peter Knight and the editor Jan A. Piotrowski for valuable comments that improved the clarity of this paper. P.L.M and N.R.I. were supported by the US National Science Foundation grant EAR-0541918. K.T.U. was supported by the BLS fund. M.P.D. was funded by a Class of 1963 Fellowship from Carleton College. K.A.B. was funded through the Faculty Research Enhancement Fund at the University of Minnesota-Morris. The authors declare no conflicts of interest.

References

Alley, R. B., Cuffey, K. M., Evenson, E. B., Strasser, J. C., Lawson, D. E. & Larson, G. J. 1997: How glaciers entrain and transport basal sediment: physical constraints. *Quaternary Science Reviews 16*, 1017–1038.

Benn, D. I. & Evans, D. J. A. 2010: *Glaciers and Glaciation*. 802 pp. Hodder Education, Abingdon.

Boulton, G. S. 1970: On the origin and transport of englacial debris in Svalbard glaciers. *Journal of Glaciology 9*, 213–229.

Brand, G., Pohjola, V. & Hooke, R. LeB. 1987: Evidence for a till layer beneath Storglaciären, Sweden, based on electrical resistivity measurements. *Journal of Glaciology 33*, 311–314.

Clark, I. D. & Fritz, P. 1997: *Environmental Isotopes in Hydrogeology*. 328 pp. CRC Lewis, New York.

Clarke, G. K. C. & Blake, E. W. 1991: Geometric and thermal evolution of a surge-type glacier in its quiescent state: Trapridge Glacier, Yukon Territory, Canada, 1969–89. *Journal of Glaciology 37*, 158–169.

Clarke, W. B., Jenkins, W. J. & Top, Z. 1976: Determination of tritium by mass spectrometric measurement of ^{3}He. *International Journal of Applied Radiation and Isotopes 27*, 217–225.

Ensminger, S. L., Alley, R. B., Evenson, E. B., Lawson, D. E. & Larson, G. J. 2001: Basal crevasse-fill origin of laminated debris bands at Matanuska Glacier, Alaska, USA. *Journal of Glaciology 47*, 412–422.

Evans, D. J. A. 2009: Controlled moraines: origins, characteristics and palaeoglaciological implications. *Quaternary Science Reviews 28*, 183–208.

Glasser, N. & Hambrey, M. J. 2002: Sedimentary facies and landform genesis at a temperate outlet glacier: Soler Glacier, North Patagonian Icefield. *Sedimentology 49*, 43–64.

Glasser, N., Hambrey, M. J., Crawford, K. R., Bennett, M. R. & Huddart, D. 1998: The structural glaciology of Kongsvegen, Svalbard, and its role in landform genesis. *Journal of Glaciology 44*, 136–148.

Glasser, N. F., Hambrey, M. J., Bennett, M. R. & Huddart, D. 2003a: Comment on Woodward *et al*. 2002. *Journal of Quaternary Science 18*, 95–97.

Glasser, N. F., Hambrey, M. J., Etienne, J. L., Jansson, P. & Pettersson, R. 2003b: The origin and significance of debris-charged ridges at the surface of Storglaciären, northern Sweden. *Geografiska Annaler 85A*, 127–147.

Hambrey, M. J., Bennett, M. R., Dowdeswell, J. A., Glasser, N. F. & Huddart, D. 1999: Debris entrainment and transport in polythermal valley glaciers. *Journal of Glaciology 45*, 69–86.

Hambrey, M. J., Huddart, D., Bennett, M. R. & Glasser, N. F. 1997: Genesis of hummocky moraines by thrusting in glacier ice: evidence from Svalbard and Britain. *Journal of the Geological Society 154*, 623–632.

Hooke, R. LeB. & Hudleston, P. J. 1978: Origin of foliation in glaciers. *Journal of Glaciology 20*, 285–299.

Hooke, R. LeB., Miller, S. B. & Kohler, J. 1988: Character of the englacial and subglacial drainage system in the upper part of the ablation area of Storglaciären, Sweden. *Journal of Glaciology 34*, 228–231.

Hubbard, B. & Sharp, M. 1995: Basal ice facies and their formation in the western Alps. *Arctic and Alpine Research 27*, 301–310.

Iverson, N. R. & Souchez, R. 1996: Isotopic signature of debris-rich ice formed by regelation into a subglacial sediment bed. *Geophysical Research Letters 23*, 1151–1154.

Iverson, N. R., Hanson, B., Hooke, R. LeB. & Jansson, P. 1995: Flow mechanism of glaciers on soft beds. *Science 267*, 80–81.

Iverson, N. R., Hooyer, T. S., Fischer, U. H., Cohen, D., Moore, P. L., Lappegard, G. & Kohler, J. 2007: Soft-bed experiments beneath Engabreen, Norway: regelation infiltration, basal slip and bed deformation. *Journal of Glaciology 53*, 323–340.

Jansson, P., Naslund, J.-O., Pettersson, R., Richardsson-Naslund, C. & Holmlund, P. 2000: Debris entrainment and polythermal structure in the terminus of Storglaciären. *In* Nakawo, M., Raymond, C. F. & Fountain, A. (eds.): *Debris-Covered Glaciers*, *September 2000*, 143–152. International Association of Hydrological Sciences (IAHS) Publication 264.

Jouzel, J. & Souchez, R. A. 1982: Melting-refreezing at the glacier sole and the isotopic composition of the ice. *Journal of Glaciology 28*, 35–42.

Kirkbride, M. & Spedding, N. 1996: The influence of englacial drainage on sediment transport pathways and till texture of temperate valley glaciers. *Annals of Glaciology 22*, 160–166.

Knight, P. G. 1997: The basal ice layer of glaciers and ice sheets. *Quaternary Science Reviews 16*, 975–993.

Kotzer, T. G., Kudo, A., Zheng, J. & Workman, W. 2000: Natural and anthropogenic levels of tritium in a Canadian Arctic ice core, Agassiz Ice Cap, Ellesmere Island, and comparison with other radionuclides. *Journal of Glaciology 46*, 35–40.

Lawson, D. E., Strasser, J. C., Evenson, E. B., Alley, R. B., Larson, G. J. & Arcone, S. 1998: Glaciohydraulic supercooling: a freeze-on mechanism to create stratified, debris-rich basal ice: I. Field evidence. *Journal of Glaciology 44*, 547–562.

Lukas, S. 2005: A test of the englacial thrusting hypothesis of 'hummocky' moraine formation: case studies from the northwest Highlands, Scotland. *Boreas 34*, 287–307.

Moore, P. L. 2009: *Dynamics of ice flow and sediment transport at a polythermal glacier terminus, Storglaciären, Sweden*. Ph.D. thesis, Iowa State University, 175 pp.

Moore, P. L., Iverson, N. R., Brugger, K. A., Cohen, D., Hooyer, T. S. & Jansson, P. 2011: Effect of a cold margin on ice flow at the terminus of Storglaciären, Sweden: implications for sediment transport. *Journal of Glaciology 57*, 77–87.

Moore, P. L., Iverson, N. R. & Cohen, D. 2009: Ice flow across a warm-based/cold-based transition at a glacier margin. *Annals of Glaciology 50*, 1–8.

Moore, P. L., Iverson, N. R. & Cohen, D. 2010: Conditions for thrust faulting in a glacier. *Journal of Geophysical Research 115*, F02005, doi: 10.1029/2009JF001307.

Östlund, G. & Lundgren, L. B. 1964: Stockholm natural tritium measurements. *Tellus 16*, 118–130.

Pettersson, R., Jansson, P., Huwald, H. & Blatter, H. 2007: Spatial pattern of the cold surface layer of Storglaciären Sweden. *Journal of Glaciology 53*, 99–109.

Rempel, A. W. 2008: A theory for ice-till interactions and sediment entrainment beneath glaciers. *Journal of Geophysical Research 113*, F01013, doi: 10.1029/2007JF000870.

Seaberg, S. Z., Seaberg, J. Z., Hooke, R. LeB. & Wiberg, D. 1988: Character of the englacial and subglacial drainage system in the lower part of the ablation area of Storglaciären, Sweden, as revealed from dye-trace studies. *Journal of Glaciology 34*, 217–227.

Souchez, R. A. & de Groote, J. M. 1985: δD and δ^{18}O relationships in ice formed by subglacial freezing: paleoclimatic implications. *Journal of Glaciology 31*, 229–232.

Souchez, R. A. & Jouzel, J. 1984: On the isotopic composition in the δD and $\delta^{18}O$ of water and ice during freezing. *Journal of Glaciology 30*, 369–372.

Strasser, J. C., Lawson, D. E., Larson, G. J., Evenson, E. B. & Alley, R. B. 1996: Preliminary results of tritium analyses in basal ice, Matanuska Glacier, Alaska, USA: evidence for subglacial ice accretion. *Annals of Glaciology 22*, 126–133.

Swift, D. A., Evans, D. J. A. & Fallick, A. E. 2006: Transverse englacial debris-rich ice bands at Kviarjokull, southeast Iceland. *Quaternary Science Reviews 25*, 1708–1718.

Uno, K. T. 2008: *A geochemical study of the origin of debris bands at Storglaciären, Sweden*, M.Sc. thesis, University of Utah, 71 pp.

Weertman, J. 1961: Mechanism for the formation of inner moraines found near the edge of cold ice caps and ice sheets. *Journal of Glaciology 3*, 965–978.

Weertman, J. 1966: Effect of a basal water layer on the dimensions of ice sheets. *Journal of Glaciology 6*, 191–207.

Woodward, J., Murray, T. & McCaig, A. 2002: Formation and reorientation of structure in the surge-type glacier Kongsvegen, Svalbard. *Journal of Quaternary Science 17*, 201–209.

Woodward, J., Murray, T. & McCaig, A. 2003: Reply to Glasser, *et al.*, 2003. *Journal of Quaternary Science 18*, 99–100.